Journal of Geoscience and Environment Protection, 2025, 13(2), 299-320
https://www.scirp.org/journal/gep
ISSN Online: 2327-4344
ISSN Print: 2327-4336

# Microclimate Indicators and Air Dust Dynamics around a Tropical Highland Open Pit Mine, Amid Progressive Ecological Rehabilitation

**Lefranc Busane Basima[1,2*], Venant Muderhwa Nshombo[1,3], Jean-Berckmans Bahananga Muhigwa[1], Cubaka Kabagale Alfred[1], Christian Kalikone[1]**

[1]Faculty of Sciences, Université Officielle de Bukavu (UOB), Bukavu, Democratic Republic of the Congo
[2]Sustainability Department, Twangiza Mining SA, Mwenga, Democratic Republic of the Congo
[3]Centre de Recherche en Hydrobiologie, Uvira, Democratic Republic of the Congo
Email: *LBasima@gmail.com

**How to cite this paper:** Basima, L. B., Nshombo, V. M., Muhigwa, J.-B. B., Alfred, C. K., & Kalikone, C. (2025). Microclimate Indicators and Air Dust Dynamics around a Tropical Highland Open Pit Mine, Amid Progressive Ecological Rehabilitation. *Journal of Geoscience and Environment Protection, 13,* 299-320.
https://doi.org/10.4236/gep.2025.132018

**Received:** January 15, 2025
**Accepted:** February 24, 2025
**Published:** February 27, 2025



## Abstract

This paper analyses microclimate parameters viz. rainfall, temperature, relative humidity, heat index, wind speed, wind direction, atmospheric pressure, dew point, air dust and air density around the Twangiza gold mine, Eastern DR Congo. Results show that in previous decades, May did not use to be a dry month as it was an integral part of the shorter rainy season and September has become drier. This depletion of May and September rainfall is a change in the study region. A significant difference was observed between both septennia (2010-2017 and 2018-2024) regarding the second rainy season (B = February-May) only at one of stations. Significant differences occurred between both septennia regarding the dry season (June-August), with more rainfall in the second septennium (2018-2024). This confirms a microclimate change in the study area, even at a range of 3 - 10 km distance, indicating patchy rains. The values of temperature and heat index increased during the second septennium; e.g. 25.3˚C max dry season 2018-2024 vs 23.4˚C dry season 2010-2017; thus differences of 1.9˚C for temperature and 1.5˚C for heat index. This is an indicator of warming in the microclimate along the quindecinnial. The results show that the mine generates seven to ten times more dust when in operations due to moving equipment and other ancillary equipment. The residential and industrial guideline limits did not change even when the mine was operational. This study has the merit of illustrating the accuracy of the best regional climate change prediction models, such as the GIZ long-term forecast for the neighbor country, Burundi, which predicted the increase of rains in the rainy season, the depletion of rains in months leading up to the dry season (August/September), implying the prolongation of the dry season. They also noted a high probability that annual average air temperatures will gradually increase.

**Keywords**

Microclimate Change, Mining, Dust

## 1. Introduction

Climate change is recognized as a global issue. The consequences of climate change for agriculture and food security in developing countries are of serious concern. Due to their reliance on rain-fed agriculture both as a source of income and consumption, many low-income countries are generally considered most vulnerable to climate change (Channing et al., 2011). It was found that in Ethiopia, the variability of rainfall and its concentration in a few months shorten the crop-growing period and constrain the production and productivity of crops, ultimately affecting food security of farmers (Habte et al., 2023). Dry spells were also found in spring and autumn. This indicated that there was a probability of risk occurrence in relation to soil moisture deficit and crop growth during the spring and autumn rainy seasons of the region (Negash & Eshetu, 2016).

In the case of Burundi, Liersch et al. (2014) have estimated that rainfall should generally increase in the eastern and southern regions of the country as well as on the central plateau with heavier rainfall. There is a high probability that annual average air temperatures will gradually increase in Burundi over the course of the 21st century. The air temperature will rise particularly during the dry season. Changes in rainfall patterns and amount of precipitation, as well as temperature, are likely to have major implications for agricultural production, particularly for crops.

Other studies from the Albertine region have provided evidence of climate change. In Rwanda, Twahirwa et al. (2022) found a considerable upward trend in the annual total precipitation for very wet days and the annual count for very heavy precipitation days. Additionally, temperature indices showed a large rise in the minimum and maximum values of daily minimum temperatures, annual minimum and maximum values of daily maximum temperatures, and the percentage of days with daily maximum temperatures for warm days. Seshaba et al. (2024) found that the majority of meteorological stations showed an increase in both hot days and nights, confirming Rwanda is warming over time, since the 1930s to 2014.

In the DRC, forecasts of average annual rainfall and temperature in the country's four climate zones point to an increase in rainfall, except in coastal areas, coastal fringe (Bas-Congo) and the extreme south, including Katanga. The details perceptible from the monthly totals clearly show a shortening of the rainy season as we move towards the south. The further south you go, Katanga, in particular, has less than 5 months of the rainy season, compared with 7 at present. In addition, the whole country will continue to be affected by thermal warming, which will continue to increase (RDC. Min. Environnement, n.d.).

Akonkwa et al. (2015) who studied climate change around Lake Kivu observed qualitative and quantitative disturbances in the variation of rainfall, a significant increase in temperature of 1.57˚C, 0.63˚C and 0.66˚C respectively at Kamembe, Gisenyi in Rwanda and Lwiro in the DRC, around Lake Kivu watershed. The relative humidity decreased significantly by 4.5% and 7% at Gisenyi and Kamembe respectively; the wind speed decreased by 3 $m \cdot s^{-1}$. These changes resulted in a decrease of 0.58 m in water level of the lake. Muhigwa (1999) argued that in the region around Bukavu, August had become a humid month, and that the very humid months had changed their ranking order: November, December, October, February, March, January and April. The rainy season starts by end August rather than September and suddenly stops, thus September becoming less and less humid. April and May rains tend to diminish. There was a highly significant increase of the average monthly temperature during the years 1990-1995 compared to 1970-1975; with the changes ranging between 0.5˚C - 1˚C and September recording a gap of 1.5˚C. The maximum temperature did not vary significantly, but the minimum temperature has witnessed a significant rise in the 1990s. The number of downpours have augmented, especially in December, which evens the annual totals, with no noticeable advantages for the farmer. The proportion of rainy days per season follows a decreasing trend and the number of sufficient rains varies.

Effects of the mining industry on the surrounding microclimate has been mentioned by various authors (Loksa, 2007; Sadeli, 2012; Worlanyo & Li, 2021; Tannor et al., 2023; Haddaway et al., 2019). Loksa (2007) argued that open cast mining involves significant changes in topography and thus influences the physical conditions of the atmosphere in the mining area and in its immediate surroundings. His results proved changes of 0.5˚C - 3.1˚C comparing temperatures of near surface ground and 2 m depth of coal mining pits in summer. Among the reasons, if one considers that the solar energy, which controls the physical processes of the atmosphere, reaches the atmosphere through the mediation of the surface; the ground surface more precisely. Its material composition is of great importance in meteorological processes. Open cast mining continuously modifies these properties. When a mining pit is deepened, open air space is created (Sumanth, Khare, & Shukla, 2020). Consequently, the air space of a mine pit tends to warm up rapidly when insolation is intense while cold air tends to accumulate in it when insolation is low and missing.

Sadeli (2012) assessed the potential impact of reforestation for the microclimate in a coal mining area, east Kalimantane and found that the mean daily temperature was lower under forest cover than open space. Solar radiation was higher in open space that in forest cover. Microclimates below forest canopies and forest openings have been studied extensively for quindecinnials (Sumanth, Khare, & Shukla, 2020).

While many factors affect dust precipitation rate, the main factors are related to wind velocity, air humidity, particulate size and dynamic shape, prevailing groundcover and density of the particle (Kuhn & Loans, 2016).

This paper focuses on the dynamics of microclimate change around a tropical highland open pit mine at the Twangiza gold mine. Alluvial gold prospecting in the Twangiza area, with a surface area of 1156 sq. Km, started in 1938 (Twangiza Gold Mine, 2007).

The current mine infrastructure was constructed in 2009. This operating open pit gold mine is located on a hilly topography averaging between 2000 and 2500 m asl with the highest surrounding hill reaching 3250 m.

Negative effects of the mine on the microclimate may be expected. However, positive effects are likely, and most probably linked with the progressive afforestation boosted by the community-based afforestation supported by the mine ecological progressive rehabilitation program (100 ha so far), which provide sensitization, tree seedlings distribution and follow up on growth. This community-based afforestation is much larger in space and cover areas from Kaziba, Luhwindja, Burhinyi and Ngweshe chiefdoms, accounting in total for 635,934-tree seedlings distributed, up to 2023, and followed up in terms of pricking and growth rate.

Such effects are analyzed in this paper, using the quindecinnial environmental monitoring data, which have been collected since 2010 at the main meteorological station and from rain gauges established, at four separate stations. The high resolution with stations just spaced 3 - 5 km will be appropriate to detect micro-climate changes (Van Vyve, 2006; da Silva et al., 2020).

The following parameters are subject to investigations in the present study: rainfall, temperature, humidity, heat index, wind direction, wind speed, dew point, air density and air dust. This study has the merit of illustrating the accuracy of the best regional climate change prediction models.

## 2. Material and Methods

### 2.1. Study Area

The Twangiza open pit gold mine is located in the Mwenga Territory, South Kivu Province, DR Congo, at 45 km south-southwest of Bukavu city, the capital of the South Kivu Province. The road access from Bukavu is at 85 Km, through the national road (RN2). Its lowest average temperature is 13 degrees Celsius while its maximum is 22 degrees with a hilly topography averaging between 1700 - 2500 m asl. However, the highest close by hill goes up to 3250 m asl (Basima et al., in press).

The mine area consists of a network of steep hills and valleys that result in a dense stream catchment area, draining in a northwesterly direction. The Mwana River to the west and the Lulimbohwe River to the east surround the ridge that the mine occupies. Both the Mwana and Lulimbohwe are fast flowing, perennial, rock mountain rivers. They converge immediately to the north of the exploration camp, at the Mwana Bridge (Bridge 6 for the mine), forming the Kadubo River that flows through Luhwindja and Burhinyi, Ngweshe, and Kasika to reach the Ulindi River, and ultimately the Congo River, of which Ulindi River is a tributary (affluent).

The following stations were selected to install plastic manual rain gauges: Exploration Camp, Plant site 5 km away; TMF area 7 km away; and Cinjira village 10 km away, as shown in Figure 1.

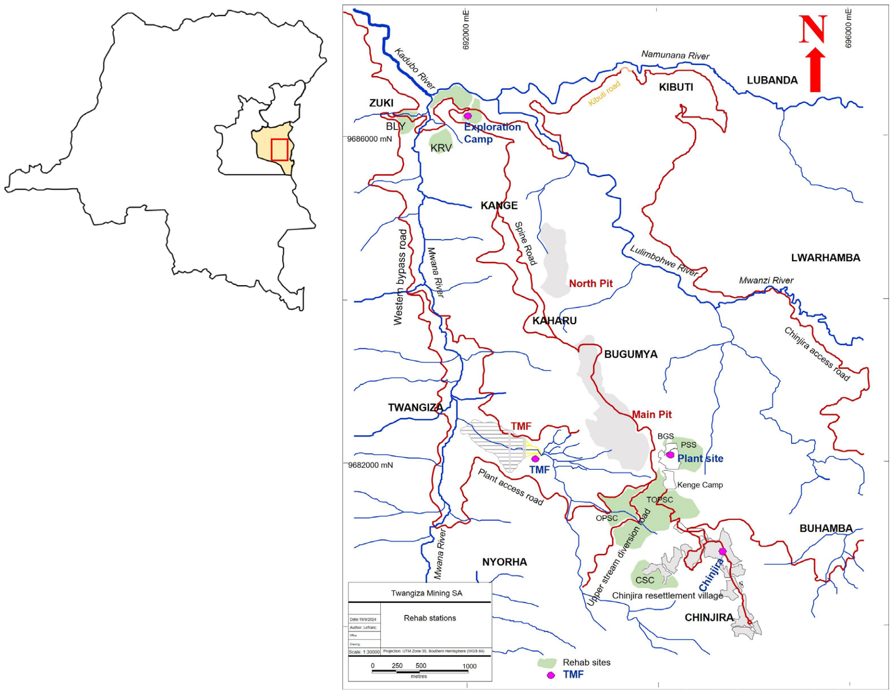


Figure 1. Location of the study area with rainfall monitoring stations (Exploration Camp, Plant site, TMF and Cinjira stations).

The topographic characteristics of the four stations indicated in Figure 1 are presented in Table 1.

Table 1. Topographic characteristic of the four stations where manual rain gauges are mounted.

| Station | Northing | Easting | Elevation (m asl) |
|---|---|---|---|
| **Cinjira** | 9681089.97 | 694496.26 | 2633.22 |
| **Plant Sitea** | 9682134.39 | 694014.01 | 2341.37 |
| **Expl.Camp** | 9686209.12 | 691906.80 | 1833.01 |
| **TMF** | 9681882.48 | 693293.31 | 2100.07 |

a. Main meteorological and rain gauge station.

## 2.2. Data Collection

### 2.2.1. Rainfall and Other Weather Data

Daily rainfall data were collected using manual rain gauges at four stations (Cinjira, Plant site, TMF site and Exploration Camp). An automated weather station Davis Vantage Pro 2, installed at the Plant site station collected for over a quindecinnial, at a 30-minute frequency interval: rainfall, wind speed, wind direction, temperature, atmospheric pressure, heat index dew point, and humidity. The data collected was transmitted to the Davis Vantage Pro 2 Wireless Receiver console, which allowed for regular and automatic downloading of data to a PC, as text files that were later converted to Excel.

#### 2.2.2. Air Dust Collection and Data Analysis

Air dust was collected using the DustWatch CC multidirectional buckets, that permits sampling of 4 different wind directions (North, South, East and West), as operated by the wind, the direction of which opens and closes the relevant sample bucket to the atmosphere.

The buckets were mounted on a frame at 2.2 meters above ground to prevent thermal interference with the precipitation phenomenon as well as the height to which particulate can be lifted with a wind of 3.0 $ms^{-1}$. The buckets were partially filled with distilled water, to which bleach was added to prevent algal growth. This media then catches and retains any precipitant reporting into the unit opening.

The dust collected was filtered through a sub-micronic pre-weighed filter using a vacuum Buchner filter arrangement. The Metler Toledo precision balance was used for weighing the filters. Once the wet filtrate has been desiccated by evaporation of any retained moisture, the filter was reweighed to calculate the collected mass.

The relevant mass classification refers to **Table 2** for historical limits (Kuhn & Loans, 2016).

**Table 2.** Historical Classification—American Standard Test Method—ASTM D1739—Dust = Milligrams/day/square meter—mg/m²/day.

| Historical S.A. Classification Department of Environmental Affairs & Tourism—updated 2011 | ASTM EQUIVALENT (mg/m²/day) | German DIN Air Quality Monthly Limit (mg/m²/day) |
|---|---|---|
| SLIGHT (< 250) | < 250 | 650—Non-industrial limit |
| MODERATE (251 to 500) | 251 - 500 | 1300—Industrial limit |
| HEAVY (501 to 1200) | 501 - 1200 | |
| VERY HEAVY (> 1200) | > 1200 | |

The fall-out dust standards from South Africa (SANS, 2011) are shown in **Table 3** and **Table 4**.

**Table 3.** Dustfall standards from South African National Standards—Four-band scale evaluation criteria for dust deposition.

| Band Number | Band description label | Dustfall rates | Comment |
|---|---|---|---|
| 1 | Residential | D < 600 | Permissible for residential and light commercial |
| 2 | Industrial | 600 < D < 1200 | Permissible for heavy commercial and industrial |

**Continued**

| | | | |
|---|---|---|---|
| 3 | Action | 1200 < D < 2400 | Requires investigation and remediation if two sequential months lie in this band, or more than three occur in a year. |
| 4 | Alert | 2400 < D | Immediate action and remediation required following the first incidence of the dustfall rate being exceeded. Incident report to be submitted to the relevant authority. |

a. (mg/m²/day), 30 Day average.

**Table 4.** Dustfall standards.

| Classification | Dustfalla | Permitted frequency of exceeding the levels. |
|---|---|---|
| Target—long-term average | 300 | Long-term average (Annual) |
| Action—residential | 600 | Three within any year, no two sequential months. |
| Action—industrial | 1200 | Three within any year, no two sequential months. |
| Alert threshold | 2400 | None. First time exceeded, triggers remediation and reporting to authorities. |

a. (mg/m²/day), averaged over 30 days.

The cross-sectional area of the buckets is a standard constant in all of the calculations representing the area over which fall-out collection has been made (0.02545 $m^2$, the internal measured diameter of the standard bucket used is 17.5 cm).

## 2.3. Data Analysis

The 30-minutes rainfall data collected from the Davis Vantage automatic weather station and the daily rainfall from rain gauges were computed over the quindecinnial 2010-2024 using the applications Jamovi 2.3.28, JASP 0.18.3 and Statistica 10. These rainfall data over the quindecinnial were used to compute the average year rainfall trends of the study area. The non-parametric one-way ANOVA (Kruskal-Wallis test) and the parametric one-way ANOVA (F-test) and T-test were computed on Jamovi 2.3.28 and JASP 0.18.3 to compare means of the quantitative weather parameters (temperature, humidity, wind, heat index, air density, dew and atmospheric pressure) by stations, septennia (2011-2017 and 2018-2024), years and seasons. The interactions between seasons and septennia were calculated as well. The Tukey test (unequal n) was used for post hoc comparisons of means. The significance level of 5% was used for decision. The decision tree (machine learning module) based on the application SPSS 23.0 was used to compute the distribution factors (independent variables) of the quantitative parameters (dependent variables). Time series were processed on Past 4.11 to analyze the trends of the quindecinnial rainfall daily data. The Man-Kendall trend test was run as well as the moving average and the smoothing plots. Multivariate analysis of the quantitative data (temperature, humidity, wind, heat index, air density, dew point and atmospheric pressure) was computed as well using PCA (Principal Component Analysis) by stations, septennia, years and seasons as grouping variables.

# 3. Results

## 3.1. Monthly and Average Year Rainfall

The rainfall recorded on a daily basis over a quindecinnial is presented in Table 5, from 2011-2024 at the Twangiza Plant site's rain gauge at an elevation of 2341 m asl. The rainy and the dry months are highlighted in color scale. The two rainy seasons are also depicted, the main one spanning from September - January, followed by the small one extended from February - April. The dry months extends from June - August.

**Table 5.** Monthly rainfall values (mm) over the quindecinnial (2011 to 2024) at the Twangiza Plant site rain gauge station.

| YEAR | J | F | M | A | M | J | J | A | S | O | N | D |
|---|---|---|---|---|---|---|---|---|---|---|---|---|
| 2011 | 179.4 | 108 | 216.4 | 41.6 | 54.8 | 62 | 24 | 29.2 | 69.2 | 113.4 | 235 | 300.1 |
| 2012 | 121.4 | 136.5 | 146.6 | 114.2 | 84.1 | 14.1 | 44.3 | 102.7 | 105.6 | 160.9 | 101.2 | 215.1 |
| 2013 | 193.6 | 126 | 291.6 | 139.9 | 12.3 | 0.4 | 0 | 37.7 | 230.9 | 88.7 | 252.7 | 223.1 |
| 2014 | 258.3 | 195.2 | 227.1 | 89.8 | 11.7 | 47.7 | 0 | 23 | 85.8 | 195.2 | 194.6 | 149.1 |
| 2015 | 159.5 | 157.4 | 179.6 | 188.8 | 25.1 | 66.5 | 0 | 0 | 104.3 | 285.2 | 259.4 | 236.6 |
| 2016 | 214.6 | 176.4 | 107.9 | 252.5 | 45.1 | 8 | 2.2 | 12 | 179.4 | 129.1 | 103.1 | 110.4 |
| 2017 | 120.1 | 163.6 | 119.1 | 13 | 34.4 | 0 | 8 | 63.3 | 142 | 119.2 | 245.3 | 116.5 |
| 2018 | 140.8 | 158.9 | 216 | 262.5 | 71.4 | 16 | 1.9 | 89.7 | 26.4 | 87.4 | 121.2 | 241.8 |
| 2019 | 150.6 | 86.4 | 221.1 | 120.8 | 35.8 | 88.5 | 19 | 30.9 | 68.4 | 162.4 | 194.8 | 333 |
| 2020 | 218.3 | 141 | 170.1 | 242.7 | 58.3 | 45.2 | 11.3 | 51.6 | 85.6 | 174.4 | 220.9 | 203.6 |
| 2021 | 285 | 117.9 | 121.8 | 126.9 | 112.8 | 50 | 16.3 | 56.5 | 137.5 | 147.8 | 137.5 | 96.2 |
| 2022 | 168.7 | 226.3 | 279 | 177.5 | 121.7 | 0.2 | 37.5 | 55.2 | 61.3 | 101.3 | 239 | 183.9 |
| 2023 | 179.5 | 213.7 | 222.9 | 155.9 | 111.7 | 27.1 | 2.3 | 4 | 284 | 157 | 175.7 | 223 |
| 2024 | 179.5 | 232.5 | 232.5 | 186.3 | 228.8 | 28.5 | 15.8 | 9.5 | 36.8 | 216.13 | 254.5 | 199.3 |

Rainier | Moderately rainier | Less rainy | Moderately dry | Drier

In decreasing order, May rains are more intensive in 2024, 2022, 2021, 2023 and 2012 as compared to the other years of the quindecinnial (80 - 120 mm).

September even recorded heavy rains in 2023, 2013 and 2016 (179 - 284 mm). January recorded more rain in 2021, 2014, 2020 and 2016 (214 - 285 mm), February was rainier in 2022 and 2023 (213 - 226 mm). In March 2013, 2022 and 2023 were rainier (222 - 292 mm). April was dryer in 2017 and 2011 (13 - 42 mm). June had more rains in 2019, 2015 and 2011 (62 - 89 mm), while July had more rains in 2012 and 2022 (37 – 44 mm) with 2013, 2014 and 2015 recording no rain (0 mm). August was generally dryer except in 2012 and 2018 (90 - 102 mm). October had the highest rainfall in 2015 (285 mm) and lower in 2013 and 2018 (87 - 89 mm). November had lower rainfall in 2018, 2016 and 2012 (101 - 121 mm). December had very high rainfall in 2019 and 2011 (300 - 333 mm).

The monthly rainfall of the average year over a quindecinnial, from 2012-2024 at the four rain gauges is shown in Table 6.

Table 6. Average monthly rainfall for the period 2012-2024 at four rain gauge stations at Twangiza.

| Month | Cinjira | Plant site | Exploration Camp | TMF |
|---|---|---|---|---|
| January | 183 | 190 | 186 | 187 |
| February | 159.4 | 160.9 | 156.2 | 160.2 |
| March | 201 | 195 | 189 | 193 |
| April | 176 | 161 | 149 | 162 |
| May | 57.3 | 57.6 | 51 | 54.6 |
| June | 14.5 | 15.2 | 12.8 | 14.1 |
| July | 8.76 | 8.95 | 11 | 7.57 |
| August | 36.3 | 34.5 | 37.4 | 34.7 |
| September | 122 | 121 | 109 | 122 |
| October | 155 | 149 | 136 | 154 |
| November | 195 | 189 | 170 | 184 |
| December | 180 | 177 | 172 | 174 |

Rainier | Moderately rainier | Less rainy | Moderately dry | Drier

The color scale shows that May, June, July and August cover the dry season. This depletion of May rainfall is a change in the study region. The rainiest month is March mainly quite close to November, then come December and January. On this regard, February, October and April are moderately rainy months, followed by September. This overall similarity between the four stations is expected because of their proximity. The mean year per station over the quindecinnial 2011-2024, which highlights that May is a dry month, having recorded around 50 mm is presented in Figure 2.

This situation which shows that May has become a dry month has been a gradual process that was already depicted a few years back.

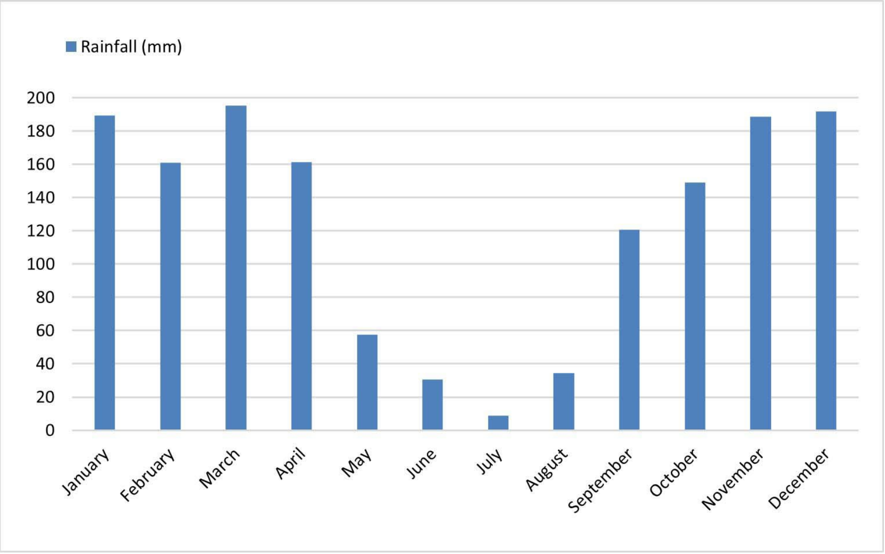


Figure 2. Average monthly rainfall at the Plant site, recorded in the period of 2012-2024.

### 3.2. Rainfall Trend at Rain Gauge Stations

Figure 3 shows a stationary and relatively stable trend with no statistically significant pattern of the rainfall over the 2011-2024 period at all of the study stations. The oscillatory pattern is by year (14 years) and seasons (dry and rainy). The Mann-Kendall trend test results are the following:

- Cinjira: S: 3406; Z: 0.80; p (no trend): 0.42 ns;
- Plant site: S: 4492; Z: 1.01; p (no trend): 0.29 ns;
- Exploration Camp: S: −68; Z: −0.02; p (no trend): 0.99 ns;
- TMF site: S: 233; Z: 0.056; p (no trend): 0.96 ns.

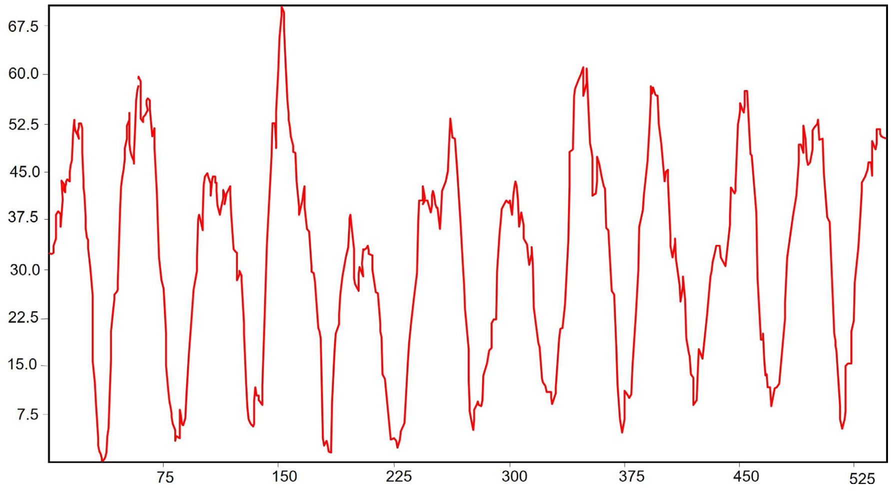


Figure 3. Smoothed trend of rainfall over the period 2011-2023 at the Plant site.

Visibly there are similar trends from 2011-2023, highlighting no difference between the two septennia. This is probably due to proximity of the huge Itombwe montane forest regarding the regional climate. Regarding the study site microclimate, a probable positive impact of the progressive afforestation is noted, boosted by the community-based afforestation supported by the mine ecological progressive rehabilitation program (100 ha so far), which provide sensitization, tree seedlings distribution and follow up on growth. This community-based afforestation is much larger in space and cover areas from Kaziba, Luhwindja, Burhinyi and Ngweshe chiefdoms accounting in total for 635,934 tree seedlings distributed and followed up, covering 757 ha within the general community (Twangiza Gold Mine, 2023).

### 3.3. Comparison of Seasons between Both Septennia Regarding Rainfall

No significant difference of daily rainfall was observed between the four stations regarding both septennia and between both septennia about the main rainy season that spans from September to January. This is probably due to the close proximity of the stations, being within 2.5 - 5 Km distance, the two furthermost stations being 7 Km a part. Though the sites are in close proximity, their elevation varies from 1800 m asl for the Exploration Camp station and 2600 m for the Cinjira station, an 800 m drop in elevation.

However, a significant difference was depicted between both septennia regarding the second rainy season (B = February-May) occurred only at the Plant site ($\bar{x}$ = 31.9 ± 28.71; versus 39.3 ± 29.07; df = 1; F = 2.86; $p$ = 0.09). This significant difference is displayed in Figure 4.

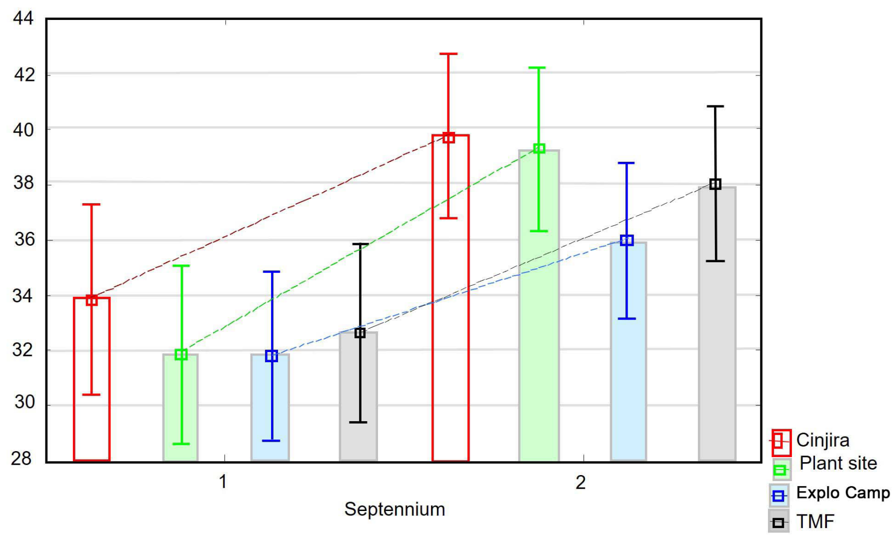


Figure 4. Mean plot multiple variables grouped by Septennium.

Also, a significant difference between both septennia regarding the dry season (June-August) occurred at 3 sites, more so at the Plant site ($\bar{x}$ = 3.9 ± 7.94 vs 8.0 ± 13.18; df = 1; F = 4.6; $p$ = 0.03); except for TMF. This is shown in Figure 5.

Peaks in rainfall recorded during the dry season at the Cinjira station are displayed in Figure 6 and Figure 7.

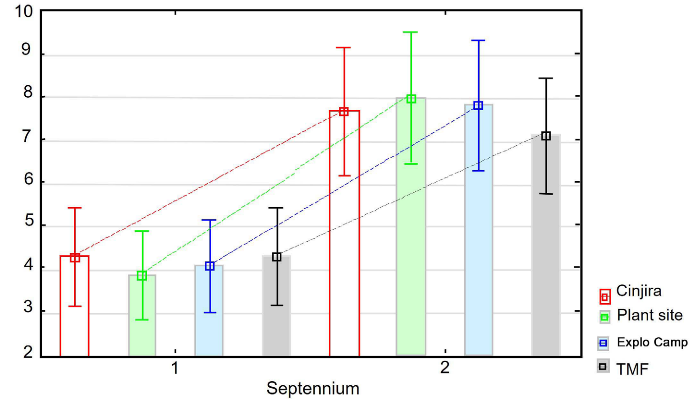


**Figure 5.** Mean plot multiple variables grouped by Septennium.

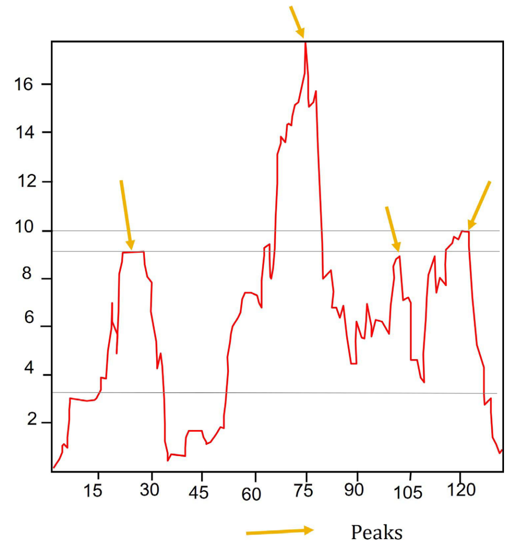


**Figure 6.** Cinjira trend of dry season rainfall.

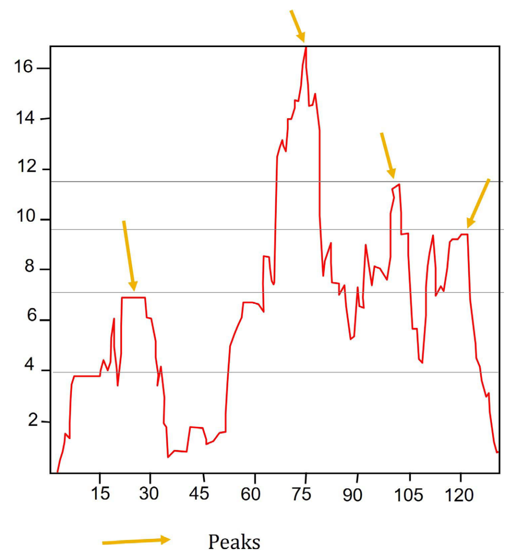


**Figure 7.** Plant site trend of quindecinnial (2012-2023) Dry season rainfall.

Peak 1 shows more rainfall during the dry season at Cinjira in septennium 2 as compared to Plant site (from 15 - 30). Peak 2 shows similar rainfall at Cinjira as compared Plant site during the 2 septennia (from 60 - 90). Peak 3 shows more rainfall at Cinjira as compared Plant site during the 2 septennia (from 91 - 106). Peak 4 shows significantly more rainfall at Cinjira as compared Plant site during the 2 septennia (from 110 - 135). The dry season had more rainfall in the second septennium (2018-2024).

Aside the manual rain gauges' data, the microclimate parameters obtained from the automated weather station at the Twangiza mine site per septennium and season are presented in Table 7.

Table 7. Descriptive statistics of the microclimate parameters from the automated weather station at Twangiza mine site per septennium (2011-2017 and 2018-2024) and season (main rainy, second rainy and dry).

| | Septennia | season | N | Mean | Lower | Upper | Median | SD | Min | Max |
|---|---|---|---|---|---|---|---|---|---|---|
| Temp_out | 1 | Dry | 26,340 | 15.4 | 15.41 | 15.47 | 14.9 | 2.43 | 9.8 | 23.40 |
| | | Rainy1 | 42,635 | 15.3 | 15.24 | 15.28 | 14.7 | 2.27 | 10.2 | 23.90 |
| | | Rainy2 | 32,864 | 15.9 | 15.86 | 15.91 | 15.4 | 2.35 | 10.3 | 24.70 |
| | 2 | Dry | 24,556 | 15.5 | 15.5 | 15.57 | 14.9 | 2.64 | 9.4 | 25.00 |
| | | Rainy1 | 44,618 | 15.3 | 15.31 | 15.35 | 14.7 | 2.40 | 9.8 | 24.70 |
| | | Rainy2 | 35,399 | 15.9 | 15.88 | 15.94 | 15.3 | 2.54 | 10.1 | 24.90 |
| Hum_out | 1 | Dry | 26,340 | 77.5 | 77.35 | 77.66 | 79 | 12.90 | 22 | 100.00 |
| | | Rainy1 | 43,060 | 85.3 | 85.23 | 85.46 | 88 | 11.90 | 27 | 100 |
| | | Rainy2 | 32,864 | 83.1 | 82.94 | 83.18 | 84 | 11.05 | 30 | 100 |
| | 2 | Dry | 24,556 | 78.9 | 78.74 | 79.07 | 80 | 13.13 | 26 | 100 |
| | | Rainy1 | 44,618 | 87 | 86.88 | 87.1 | 91 | 11.70 | 43 | 100 |
| | | Rainy2 | 35,399 | 86 | 85.83 | 86.06 | 89 | 11.10 | 31 | 100 |
| Dew_Point | 1 | Dry | 26,340 | 11.3 | 11.26 | 11.31 | 11.4 | 1.96 | -2.6 | 16.30 |
| | | Rainy1 | 42,635 | 12.6 | 12.6 | 12.63 | 12.6 | 1.71 | 0.6 | 19.10 |
| | | Rainy2 | 32,864 | 12.8 | 12.83 | 12.87 | 12.9 | 1.77 | 1.2 | 19.60 |
| | 2 | Dry | 24,556 | 11.6 | 11.62 | 11.67 | 11.8 | 1.88 | -2.4 | 16.90 |
| | | Rainy1 | 44,618 | 13 | 12.99 | 13.01 | 13 | 1.57 | 2.9 | 19.90 |
| | | Rainy2 | 35,399 | 13.4 | 13.39 | 13.42 | 13.4 | 1.58 | 1.5 | 18.50 |
| windHI_Speed | 1 | Dry | 19,619 | 14.7 | 14.55 | 14.8 | 12.9 | 9.07 | 1.6 | 54.70 |
| | | Rainy1 | 31,666 | 12.9 | 12.8 | 12.99 | 11.3 | 8.64 | 1.6 | 67.60 |
| | | Rainy2 | 26,528 | 15.6 | 15.54 | 15.77 | 12.9 | 9.86 | 1.6 | 78.90 |
| | 2 | Dry | 14,024 | 13.5 | 13.37 | 13.66 | 12.9 | 8.69 | 1.6 | 51.50 |
| | | Rainy1 | 21,016 | 10.9 | 10.82 | 11.04 | 8 | 8.30 | 1.6 | 51.50 |
| | | Rainy2 | 19,349 | 11.9 | 11.8 | 12.04 | 11.3 | 8.25 | 1.6 | 61.20 |

**Continued**

| | | | | | | | | | | |
|---|---|---|---|---|---|---|---|---|---|---|
| Heat_Index | | Dry | 26,340 | 15.3 | 15.28 | 15.33 | 14.7 | 2.36 | 10.1 | 23.2 |
| | 1 | Rainy1 | 42,635 | 15.3 | 15.29 | 15.33 | 14.7 | 2.26 | 10.6 | 23.8 |
| | | Rainy2 | 32,864 | 16 | 15.92 | 15.97 | 15.4 | 2.41 | 10.6 | 25.6 |
| | | Dry | 24,556 | 15.4 | 1542 | 15.49 | 14.8 | 2.58 | 9.7 | 24.7 |
| | 2 | Rainy1 | 44,618 | 15.4 | 1541 | 15.45 | 14.8 | 2.38 | 10.1 | 24.2 |
| | | Rainy2 | 35,399 | 16.1 | 16 | 16.07 | 15.4 | 2.57 | 10.3 | 24.8 |

The septennium grouping for the automated weather station parameters are highlighted in Figure 8.

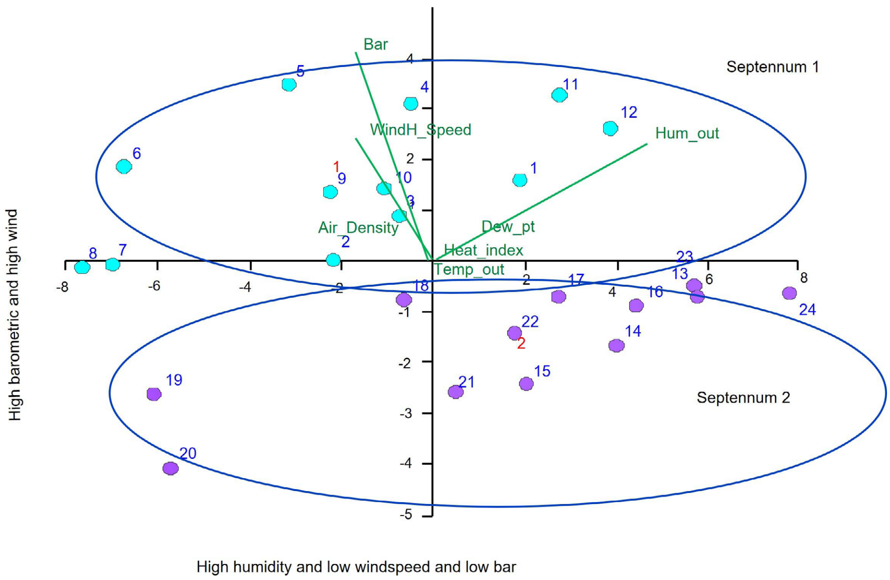


**Figure 8.** Septennium grouping for weather parameters under study.

This grouping is summarized in Table 8.

**Table 8.** Septennium grouping for weather parameters under study.

| Septennium | Lower values of | Higher values of |
|---|---|---|
| 1 = 2011-2017 | | Barometric pressure, wind speed and humidity |
| 2 = 2018-2024 | Wind speed and barometric pressure | Temperature, heat index and dew point |

The barometric pressure, wind speed and humidity values were higher during the first septennium (2011-2017) and they decreased during the second septennium (2018-2024) (Figure 8 and Table 8). However, the values of temperature, heat index and dew point increased during the second septenuum; e.g 25.3˚C max dry season 2018-2024 vs 23.4˚C dry season 2010-2017; thus differences of 1.9˚C for temperature and 1.5˚C for heat index were observed. This is an indicator of warming in the microclimate along the quindecinnial.

The Kruskal-Wallis test shows a significant difference of temperature between the two septennia (X2 =3.69; df = 1; $p = 0.05$). The parametric ANOVA also shows a significant difference between seasons ($p < 0.001$) and there is a significant interaction between septennium and season ($p = 0.04$).

There is a highly significant difference between the dry season and the main rainy season, the dry season and the second rainy season and between the 2 rainy seasons ($p < 0.001$). This highly significant difference between the three seasons is observed during the 2 septennia.

The max wind speed variable distribution mainly varied by the septennium ($\bar{x}$ = 13.3 ± 9.01 m/s; n = 132 357) followed by the month and year. During the first Septennium, the average high wind speed was 14.3 ± 9.26 m/s; n = 77 813. In the second Septennium, the average max wind speed was 11.9 ± 8.44 m/s; n = 56 544. The slowest max winds were noted in April, December and January 2024 ($\bar{x}$ = 5.9 ± 4.21; n = 829) and in June, September 2023 ($\bar{x}$ = 7.9 ± 6.07).

There is a highly significant difference between values of max wind speed between the 2 septennia, the months and an interaction between septennia and months.

Figure 9 shows the average high wind speed by season during both septennia.

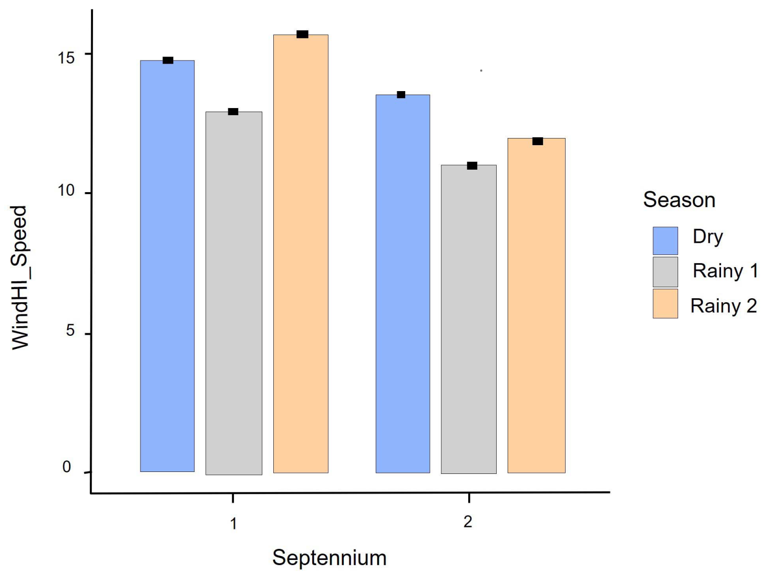


Figure 9. Average wind speed recorded by seasons during both septennium.

During the dry season, the maximum wind speed values were highest 2014. In the main rainy season, the wind speed was highest in 2014 as well. The high wind speed peaked up during the second rainy season, only in 2011, 2014 and 2017.

The most frequent wind direction in the study area is ENE, NE followed by NNE during the first septennium (2011-2017). During the second septennium, the predominant wind direction is NNE followed by N.

Regarding dust fall-out precipitation, there was a highly significant difference between 2017 and 2023 ($p < 0.001$). For the difference between 2017 and 2023, the dust fallout has respectively 420.7 and 42.6 (mg/m$^2$/day), thus a tenfold difference. A significant difference was observed for dust intensity between 2018 and 2023 ($p = 0.05$), respectively 308 and 42.6, thus a seven-fold difference. Mining activities were halted in December 2019, a reason of the decrease in dust fallout. A similar difference between 2017 and 2023 was observed in the southern direction, respectively 402.5 and 55.5, a seven-fold difference. A highly significant difference was observed between 2018 and 2023 with respectively 353.4 and 55.5, showing again a six-fold difference. In the eastern direction, dust fallout intensity in 2017 was highly significantly more than 2023, with a tenfold difference (497.5 vs 47.8). The trend was similar in the western direction, the dust fallout being 9 times more intensive in 2017 than 2023 (431.2 vs 46.0). The results show that when operational, the mine produced 7 to 10 times more dust that when not operational, which is attributed to mobile and mineral extracting equipment. However, the results show that whatever the situation, the dust level residential limit was not exceeded.

# 4. Discussion

## 4.1. Correlations between the Meteorological Parameters

The correlation factors describing the meteorological parameters at the Twangiza site are presented in Table 9.

**Table 9.** Correlation factors describing meteorological parameters at the Twangiza site.

| | Factor 1 | Factor 2 | Factor 3 |
|---|---|---|---|
| Factor 1 | 1 | 0.071 | −0.52 |
| Factor 2 | 0.071 | 1 | −0.406 |
| Factor 3 | −0.52 | −0.406 | 1 |

The meteorological parameters are grouped into 3 assemblages as shown in Figure 10: 1) Heat Index and relative humidity. Minimum, high and average temperature. 2) Dew point with relative humidity 3) Air pressure and Atmospheric pressure and air density. The Heat component negatively affected relative humidity, i.e. when temperature and heat increased, relative humidity diminished ($\gamma = -0.52$). Also when the heat and temperature increased, the air pressure diminished. When the air pressure increased, the dew point decreased ($\gamma = -0.41$). Temperature variance was utterly explained by component 1 (100%) alike heat index and maximum and minimum temperature, but negatively affected relative humidity. Factor 2 strongly explained the variance of the Dew point (94%) but less so for the relative humidity (41%). The air density and barometric pressure variances were both explained by component 3 (64% and 54.5%). Actually, the 3 components explained up to 92% of the overall variances.

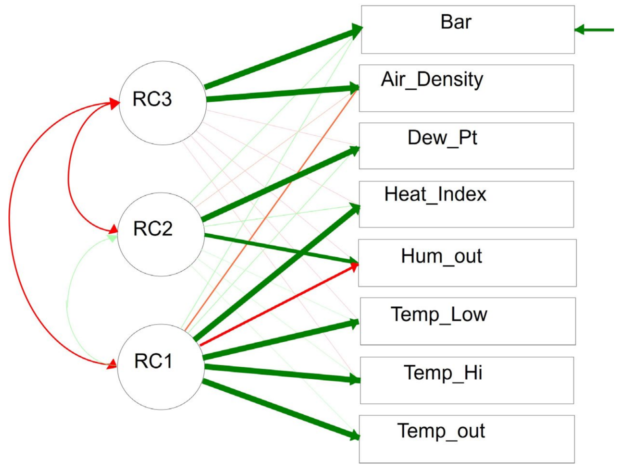


**Figure 10.** Meteorological parameter assemblages in the study area (path diagram).

In line with the current results, Allarakha (2024) stated that Temperature is another factor that affects air density. As the temperature increases, air molecules move faster and spread further apart when colliding. Higher temperatures and lower air pressure at high altitudes reduce air density. Increasing altitude decreases air pressure. Air becomes denser as air pressure increases.

In the Twangiza area, which extends from 1700 - 3000 m asl, the weather forecast around the mine site is unpredictable with the day weather changing frequently and suddenly to the extent that visitors and the general public always gear themselves as changes may be experienced at any time, as if they were experiencing all the seasons in just a day. In fact, it is known that a rise in barometric pressure is generally considered an improvement in the weather or clear skies, while low barometric pressure may mean worsening weather, and rain or snow, within a day or two. When barometric pressure is high, the air is heavy and dense and stays close to the earth's surface, allowing the sun to shine. Low pressure allows the air to rise and form clouds, and produce rain, or snow if it is cold enough. Low pressure also produces high winds because air can move more easily, and when it happens over a warm ocean, it can generate a storm (WMO, 2023).

## 4.2. Trends of Rainfall and Heat

Barometric pressure, wind speed and humidity values were higher during the first septennium (2011-2017) and they decreased during the second septennium (2018-2024). However, the values of temperature, heat index and dew point increased during the second septennium. Differences of 1.9˚C for temperature and 1.5˚C for heat index were observed. This is an indicator of warming in the area along the quindecinnial. Supporting this result, Liersch et al. (2014) predicted in neighboring Burundi that, although rainfall is expected to increase in the rainy season, the months leading up to season (August/September) are likely to be drier. Some of the models used predict a probable prolongation of the dry season. In previous decades, before 1984, May did not use to be a dry month as it was an integral part of the shorter rainy season and September has become drier. This depletion of May and September rainfall is a change in the study region (Muhigwa, 1999).

Ngarukiyimana et al. (2021) found that the spatial distributions of $T_{max}$ and $T_{min}$ represent a significant warming trend over the whole country notably since the early 1980s. Surprisingly, $T_{min}$ increased at a faster rate than $T_{max}$ in R3 (0.27˚C vs. 0.07˚C/decade in March-to-May) and (0.29˚C vs. 0.04˚C/decade in October-to-December), resulting in a significant decrease in the DTR. This is another confirmation of warming in Rwanda from 1961 to 2014 within 3 elevation regions: 1000 - 1500 m; 1500 - 2000 m and ≥ 2000 m).

Engdaw et al. (2021) located the increase in temperature and heat in Africa around 2016 as compared to 2010. According to them, most data sets agree in identifying 2010 as a peak heat year over Northern and Western Africa while Eastern and Southern Africa experienced the highest heat wave occurrence in 2016. Their Results clearly reveal that heat wave occurrences have emerged from natural climate variability in Africa. In addition to temperature, also humidity, wind and incident radiation play a role in altering the occurrence and characteristics of heat waves (Engdaw et al., 2021).

### 4.3. Variability and Intermittence of Rainfall between Nearby Places

Significant differences occurred between both septennia regarding the dry season (June-August), with more rainfall in the second septennium (2018-2024). This confirms a microclimate change in the study area, even at a range of 3 - 10 km distance, indicating intermittent rains. Van vyve (2006), who studied the spatial variation in rainfall in southern Niger (non-arid) tropical climate, showed over a radius of 1 - 20 km that the best way to manage rainfall-related risks in agriculture is to spread the fields around the village; since the probability of rainfall in two places a few kilometers apart is highly random. From a spatial point of view, she observed a great variability in annual totals; e.g. for the year 2000, she noted a zone of around 300 mm rainfall spaced about 5 km apart from an area where annual rainfall exceeded 500 mm. For some years (2000, 2003 and 2004), She observed a limited number of large wetter and drier zones. In 2001 and 2005, on the other hand, the annual totals were organized into limited wetter and drier zones, which are very heterogeneously organized. She noted that farmers had been spreading their fields around the village for a long time. They have always been aware of the risks associated with variability of rainfall in their region.

This difference of rainfall levels between nearby places is commonplace in various regions and climates, as shown by local or national high-resolution precipitation analyses, especially at the boundary of any neighbor isohyets. da Silva et al. (2020) illustrated such intermittence of rains in a reservoir catchment in Brazil.

A microclimate is a small area that has different atmospheric conditions than the surrounding area (Camus, 2017). Ellis & Eaton (2021) indicated that microclimates can be found in most places but are most pronounced in topographically dynamic zones such as mountainous areas, as the case of Twangiza, but also on islands, and coastal areas. Agele (2000) argued that opencast mining activities, alike in Twangiza, do cause soil disturbance and produce changes in the concentrations of toxic elements, dusts, biogenic gases and microclimatic gradients. These gradients in microclimate have implications for leaf to air vapor pressure differentials that control plant water relations and energy balances. There is therefore high irradiance, soil water deficits, high temperatures and vapor pressure deficits, variable substratum depths and toxic levels of some minerals (Agele, 2000).

### 4.4. Dust Emissions

The results show that when operational, the mine produced 7 to 10 times more dust that when not operational, which is attributed to mobile and mineral extracting equipment. Momoh et al. (2013) observed that suspended particulate matter in the air ranged from 60.25 to 1820.45 μg/m$^3$ at the Mukula mine in Limpompo, South Africa. Such measure includes wet drilling and blasting, sprinkling of water on the mine roads and planting of vegetation around the mines and neighboring communities. Dayda (2024) indicated that during many of the extraction and processing processes related to the production and processing of rock and mineral products, dust particles are created and can become airborne. There are three primary sources of dust in mines: drilling and blasting, loading and hauling, and crushing and grinding. As shovels scrape rock and trucks cross complex terrain, this activity generates a lot of dust. The movement of these trucks and transferring material to conveyor belts continues the cycle of dust creation, putting workers and anyone nearby in danger. Crushers break down rocks into smaller fragments, whereas grinding means the reduced size of the crushed materials, which gives fine products than crushing. Each step releases a fine dust cloud, contaminating the air and posing inhalation risks.

## 5. Conclusion

This study took place around the Twangiza gold mine, South Kivu, DRC. Various climate changes were observed. May has become an integral part of the dry season, unlike the situation in previous decades, with an impact on agriculture and animal husbandry by providing information to farmers and decision makers. Microclimate changes are indicated by significant variations in the shorter rainy season (February-May) and in the dry season (June-August), just within a range of 3 - 10 km distance, indicating patchy rains.

The barometric pressure, wind speed and humidity values were significantly decreased during the last decade, unlike temperature and heat index which increased. This is an indicator of warming in the microclimate along the quindecinnial. It is shown that the mine generates seven to ten times more dust when in operations due to moving equipment and other ancillary equipment. The residential and industrial guideline limits did not change even when the mine was operational. This study sheds light on the accuracy of the best regional climate change prediction models, such as the GIZ long-term forecast for the neighbor country, Burundi. They predicted that, although rainfall is expected to increase in the rainy season, the months leading up to season (August/September) are likely to be drier. They also noted a high probability that annual average air temperatures will gradually increase in Burundi over the course of the 21st century. The air temperature would rise particularly during the dry season.

Future research perspectives will target a larger geographic extension to confirm the regional climate changes.

## Authorization

This paper was allowed for publication by Twangiza Mining SA through the authorization letter dated December, 2023.

## Acknowledgements

The authors are grateful to the Twangiza Gold Mine management team, through its General Manager, Mr. K Zhang who granted permission for and encouraged this work to be conducted. This work would have not been materialized without the appreciated efforts made by Martin Chokola, David Mushagalusa, Musafiri Mulukwa and Dieudonné Kayeye from the mine Sustainability department who helped collect data from stations and file them appropriately. Many thanks to Arsene Bahane for the conducting all required surveys and DTM information. Eric Mbale is thanked for having fixed the vaccum Buchner filter arrangement, allowing for continued dust filtering and weighing.

## Conflicts of Interest

The authors declare no conflict of interest for this paper.

## References

[TGM] Twangiza Gold Mine (2007). *Annual Report of Activities*.

[TGM] Twangiza Gold Mine (2023). *Environmental Annual Rapport*.

Agele, S. O. (2000). *Degraded Opencast Minelands in Tropical Environments: Their Peculiar Features in Revegetation Efforts to Restore Functional Ecosystems. Microclimate and Plant Stress in the Reclamation of Abandoned Minelands. 1. Site Factors and Plant Species and Structure (Project Report)*.

Akonkwa, B., Muhigwa, B., Montcho, S. A., Nshombo, M., & Laleye, P. (2015). Climate Change and Its Impact on the Fisheries in Lake Kivu, East Africa. *Journal of Biodiversity and Environmental Sciences, 6,* 312-327.

Allarakha, S. (2024). *What Is Barometric Pressure? How Does Barometric Pressure Affect Humans*? https://www.medicinenet.com/how_does_barometric_pressure_affect_humans/article.htm

Basima, L. B., Nshombo, V. N., Muhigwa, J. B., Kalikone, C., & Vualu, P. (in press). *Surface* *and Groundwater Quality and Flow Dynamics around a Tropical Highland Open Pit Mine, amid Progressive Ecological Rehabilitation*.

Camus, J. (2017). *9 Examples of Microclimate*. https://sotoga.com/en/microclimate

Channing, A., Will, F., Ken, S., & Thurlow, J. (2011). *Climate Change, Agriculture, and Food Security in Tanzania*. WIDER Working Paper, No. 2011/52.

da Silva, R. M., Santos, C. A. G., da Costa Silva, J. F. C. B., Silva, A. M., & Brasil Neto, R. M. (2020). Spatial Distribution and Estimation of Rainfall Trends and Erosivity in the Epitácio Pessoa Reservoir Catchment, Paraíba, Brazil. *Natural Hazards, 102,* 829-849. https://doi.org/10.1007/s11069-020-03926-9

Dayda, K. (2024). *Dust Control in Mines: Methods, Sources, Solutions. Oizom.com. Redefining Resources*.

Ellis, C. J., & Eaton, S. (2021). Microclimates Hold the Key to Spatial Forest Planning under Climate Change: Cyanolichens in Temperate Rainforest. *Global Change Biology, 27,* 1915-1926. https://doi.org/10.1111/gcb.15514

Engdaw, M., Hegerl, C., Ballinger, G., & Steiner, A. (2021). Changes in Temperature and Heat Waves over Africa Using Observational and Reanalysis Data Sets. *International Journal of Climatology, 42,* 1165-1180.

Habte, A., Worku, W., Mamo, G., Ayalew, D., & Gayler, S. (2023). Rainfall Variability and Its Seasonal Events with Associated Risks for Rainfed Crop Production in Southwest Ethiopia. *Cogent Food & Agriculture, 9,* Article ID: 2231693. https://doi.org/10.1080/23311932.2023.2231693

Haddaway, N. R., Cooke, S. J., Lesser, P., Macura, B., Nilsson, A. E., Taylor, J. J. et al. (2019). Evidence of the Impacts of Metal Mining and the Effectiveness of Mining Mitigation Measures on Social-Ecological Systems in Arctic and Boreal Regions: A Systematic Map Protocol. *Environmental Evidence, 8,* Article No. 9. https://doi.org/10.1186/s13750-019-0152-8

Kuhn, G. F., & Loans, C. (2016). *DustWatch Manual—Sampling & Assessment Procedure Manual Including Risk Assessment and Safety, Health, Environment and Quality Plan*. https://www.dustwatch.com

Liersch, S., Rivas, R., & Fritzsche, K. (2014). *Rapport sur le changement climatique au Burundi: Résumé à l'intention des décideurs*. GIZ & Min. Env. Burundi.

Loksa, G. (2007). Variations in Microclimate Modified by Open-Cast Mining: Case Studies from Hungary. *Geografia Fisica e Dinamica Quaternaria, 30,* 215-218.

Momoh, A., Mhlongo, S. E., Abiodun, O., Muzerengi, C., & Mudanalwo, M. (2013). Potential Implications of Mine Dusts on Human Health: A Case Study of Mukula Mine, Limpopo Province, South Africa. *Pakistan Journal of Medical Sciences, 29,* 1444-1446. https://doi.org/10.12669/pjms.296.3787

Muhigwa, J. B. (1999). *Analyse des perturbations dans le régime pluviométrique du Sud Kivu durant les 50 dernières années* (pp. 112-121). Mus. Roy. Afr. Centr. Dépt. Géol. Min. Rapp. Ann. 1997 et 1998.

Negash, W., & Eshetu, Y. (2016). Analysis of Rainfall Variability and Farmers' Perception towards It in Agrarian Community of Southern Ethiopia. *Journal of Environment and Earth Science, 6,* 99-107.

Ngarukiyimana, J. P., Fu, Y., Sindikubwabo, C., Nkurunziza, I. F., Ogou, F. K., Vuguziga, F. et al. (2021). Climate Change in Rwanda: The Observed Changes in Daily Maximum and Minimum Surface Air Temperatures during 1961-2014. *Frontiers in Earth Science, 9,* Article ID: 619512. https://doi.org/10.3389/feart.2021.619512

RDC. Min. Environnement (n.d.). *Les changements climatiques en République Démocra-*

*tique du Congo: État de lieux et perspectives dans le cadre de l'ANCR* (19 p.). Autoévaluation Nationale des Capacités à Renforcer.

Sadeli, I. (2012). The Impact of Revegetation on Microclimate in Coal Mining Areas in East Kalimantan. *Journal of Environment and Earth Science, 2,* 90-98.

Seshaba, P., Singirankabo, E., & Nsabimana, D. (2024). Analysis of Extreme Temperature Variability in Rwanda. *Journal of Atmospheric Science Research, 7,* 74-89. https://doi.org/10.30564/jasr.v7i1.6107

South African National Standards (2011). *SANS1929: 2011 Edition 2*.

Sumanth, C., Khare, M., & Shukla, K. (2020). Numerical Modelling of PM10 Dispersion in Open-Pit Mines. *Chemosphere, 259,* Article ID: 127454. https://doi.org/10.1016/j.chemosphere.2020.127454

Tannor, S. J., Borgemeister, C., Addo–Danso, S. D., Greve, K., & Tischbein, B. (2023). Climate Variability and Mining Sustainability: Exploring Operations' Perspectives on Local Effects and the Willingness to Adapt in Ghana. *SN Business & Economics, 3,* Article No. 141. https://doi.org/10.1007/s43546-023-00515-3

Twahirwa, A., Oludhe, C., Omondi, P., Rwanyiziri, G., Ndakize, S., & Guhirwa, S. (2022). Analysis of Climate Change Indices in Musanze District, Rwanda. *Journal of Climate Change and Sustainability, 4,* 17-25. https://doi.org/10.20987/jccs.03.06.2022

Van Vyve, N. (2006). *Caractérisation de la variabilité spatio-temporelle de la pluie au Fakara, Niger. Bio-Ing* (p. 46). Thesis, Université Catholique de Louvain.

WMO (2023). *Africa Suffers Disproportionately from Climate Change*. https://wmo.int/news/media-centre/africa-suffers-disproportionately-from-climate-change

Worlanyo, A. S., & Li, J. F. (2021). Evaluating the Environmental and Economic Impact of Mining for Post-Mined Land Restoration and Land-Use: A Review. *Journal of Environmental Management, 279,* Article ID: 111623. https://doi.org/10.1016/j.jenvman.2020.111623